URSI GASS 2020, Rome, Italy, 29 August - 5 September 2020

A Design Scheme for Arbitrary 3-D Caustic Beam Field Patterns

Gabriel Lasry, Timor Melamed, and Yaniv Brick
School of Electrical and Computer Engineering, Ben-Gurion University of the Negev 8410501, Beer Sheva, Israel

Abstract

An algorithm for designing an aperture field that radiates caustic (Airy-beam type) beams along a predefined 3-D beam trajectory in free-space, with arbitrary curvature and torsion is presented. The predefined beam-axis trajectory sets the aperture field's phase to form a smooth caustic surface. The aperture amplitude distribution is constructed to manipulate both the on-axis intensity profile and the off-axis beam-width, via an iterative procedure. Once the aperture distribution is calculated, the radiation from a finite sampled aperture is computed numerically using a fast numerical technique. The algorithm is demonstrated for the case of a helical trajectory beam.

1 Introduction

The topic of curved (sometimes termed "accelerating") beam design has received significant attention in recent years. These so-called beams are field patterns with intensity profiles that peak along curved trajectories and are of a weakly-diffractive nature. Such patterns have been shown useful for various applications. These include particle manipulation, super-resolution imaging, plasmon excitation, light-sheet microscopy, optical coherence tomography, and plasma-channel generation, to name but a few [1-6]. These patterns are formed by directing energy, produced by a radiating aperture, to positions along a curved caustic surface. To produce such field patterns, corresponding field distributions on the aperture should be designed, in accordance with the desired pattern's peak intensity trajectory and other field characteristics. To that end, a technique should be developed, with the goal of optimizing the aperture distribution. Ideally, these aperture fields should be able to produce caustic beams (CBs) with complex desired features.

This work focuses on the design of an aperture field which is *close* to the desired one, and is therefore expected to enable convergence of the optimization algorithm. Natural candidates for such an initial solution are source distributions that give rise to CB patterns that follow the desired trajectory. Early works on the design of CBs, such as that in [7], focused on the Airy-type caustic beam. These beams were produced by using finite energy Airy functions as aperture distributions. The caustic mechanisms governing the Airy beam were studied analytically in [8], and laid the foundation for the development of more general design techniques, suitable to broader classes of CBs. These propose to use a ray-field description of the desired pattern, followed by back-tracing the rays, to form the pertinent aperture field distribution [9]. The ray description enables the analytical calculation of the aperture field's phase and amplitude distributions. Specifically, the technique in [9] is capable of producing caustic beams along arbitrary trajectories in 2-D, which are not of any particular spatial symmetry.

In this paper we extend the methodology in [9] to the 3-D case of beam trajectories with arbitrary *curvature* and *torsion*. The work also addressed the issue of controlling certain features of the intensity profile, such as the beam-width and the peak intensity profile along the beam axis. In the following section we describe the proposed method, demonstrate it via an example, and finally we discuss its role within optimization techniques in a follow-up research.

2 Problem Definition

Given an arbitrary trajectory in a 3-D domain

$$\mathbf{r}_{\mathrm{b}}(\sigma) = [x(\sigma), y(\sigma), z(\sigma)], \tag{1}$$

with $\sigma \in [\sigma_{\min}, \sigma_{\max}]$ denoting the arc length along the beam-axis trajectory, we aim at designing a source (aperture field) in the $z = 0$ plane that produces a 3-D beam-field, with a *beam-axis* that follows this curved trajectory, in free-space. The beam-field's desired transverse width is denoted $W_{\mathrm{b}}(\sigma)$ (see figure 1) and $I_{\mathrm{b}}(\sigma)$ denotes the desired intensity profile along the beam-axis. The designed aperture field, denoted $u_0(x', y')$, is sought in the form of a ray-field

$$u_0(x', y') = A(x', y') \exp[-jkS(x', y')], \tag{2}$$

where $k = \omega/c$ is the wavenumber, with c being the free-space wave velocity. Also in (2), (x', y') are coordinates in the $z = 0$ plane, and A and S are identified as the aperture field's *amplitude* and *phase* (Eikonal) distributions, respectively. In section 3, we present a method for designing the two functions, A and S, given the desired beam-axis trajectory, $\mathbf{r}_{\mathrm{b}}(\sigma)$, intensity, $I_{\mathrm{b}}(\sigma)$, and beam-width, $W_{\mathrm{b}}(\sigma)$. The design approach relies on the observation that the radiated field's intensity can be confined to the vicinity of a geometrically complex trajectory $\mathbf{r}_{\mathrm{b}}(\sigma)$, if the aperture phase, asymptotically, gives rise to a caustic surface that contains $\mathbf{r}_b(\sigma)$. The methodology is summarized in the following section.

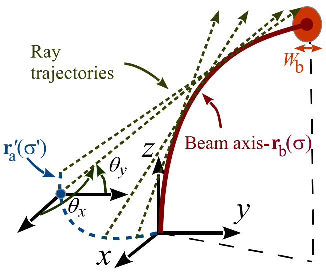

Figure 1. Mapping the beam-axis to the aperture curve. Each point on the beam-axis $\mathbf{r}_b(\sigma)$ is mapped to a point $\mathbf{r}_a'(\sigma)$ over the aperture from which the ray is emanating in the direction $[\theta_x(\sigma), \theta_y(\sigma)]$.

3 Methodology

3.1 Aperture Phase Distribution

The aperture phase dictates the beam-axis trajectory. This phase is determined by associating, with each point on the aperture, a ray, such that a caustic is formed over a surface containing the beam-axis $\mathbf{r}_b(\sigma)$. The ray from point (x', y') on the aperture is emanating in the direction [10]

$$\nabla' S(x', y') = \begin{bmatrix} \cos\theta_x(x', y') \\ \cos\theta_y(x', y') \end{bmatrix}, \quad (3)$$

where $S(x'y')$ is the phase in (2) and $\theta_{x,y}$ are the angles formed between the ray and corresponding axes (see figure 1). From each point $\mathbf{r}_b(\sigma)$ along the beam-axis we follow the tangent ray back to the emanating point on the aperture, denoted $\mathbf{r}_a'(\sigma)$. This procedure maps points on the axis to points on the curved trajectory $\mathbf{r}_a'(\sigma)$ in the aperture, and corresponding (rays') angles. Next, we define the local curve coordinates, (σ', n'), on the aperture plane, where σ' is the arc length along the curve $\mathbf{r}_a'(\sigma')$ and n' denotes the distance of a point (x', y') from $\mathbf{r}_a'(\sigma')$ (in the normal direction), with corresponding unit vectors, $\hat{\boldsymbol{\sigma}}'$ and $\hat{\mathbf{n}}'$ (see figure 2). The parameter $\sigma \in [\sigma_{\min}, \sigma_{\max}]$ can be mapped to $\sigma' \in [0, \sigma'_{\max}]$. Using these definitions, we first evaluate the phase, $S(\sigma', n')$, along the curve $\mathbf{r}_a'(\sigma')$, i. e., $S(\sigma', 0)$, and then, the phase is extended to other points on the aperture. In order to satisfy (3) for point over $\mathbf{r}_a'(\sigma')$, we extend the phase $S(\sigma', 0)$ for small n' values via

$$S(\sigma', n') = S(\sigma', 0) + n'\hat{\mathbf{s}}(\sigma') \cdot \hat{\mathbf{n}}'(\sigma'). \quad (4)$$

The phase in (4) forms a smooth caustic surface that passes through the beam-axis.

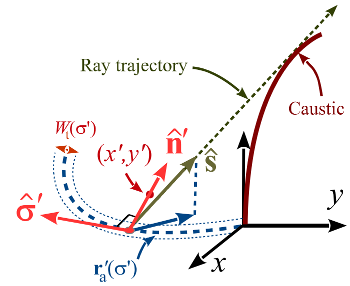

Figure 2. The local curve coordinates, (σ', n'). For each point over the planar curve $\mathbf{r}_a'(\sigma')$ we project the ray direction $\hat{\mathbf{s}}$ onto the unit vectors $\hat{\mathbf{t}}'$ and $\hat{\mathbf{n}}'$ and reconstructs the aperture field accordingly.

3.2 Aperture Amplitude Distribution

In order to manipulate and control the beam-width, we apply the local beam coordinates that are associated with the beam-axis in (1). Denoting σ the arc length along the beam-axis trajectory, the beam local coordinates are defined by the unit vectors $\hat{\mathbf{t}}(\sigma), \hat{\mathbf{n}}(\sigma)$, and $\hat{\mathbf{n}}_b$, being the tangent, normal, and bi-normal to $\mathbf{r}_b$ directions. Since $\mathbf{r}_b$ is a trajectory over a caustic surface, we identify the mechanism of enhanced intensity along the local coordinate n as the caustic local structure. Therefore, in the proposed method, control over the width of the beam intensity in the local $\hat{\mathbf{n}}$ direction is not possible. However, the beam-width in the transverse n_b coordinate and the intensity profile along σ are controllable. In our implementation, we design the aperture field amplitude in (2) to be of the general form

$$A(x', y') = w_t(n', \sigma') w_l(\sigma'). \quad (5)$$

The beam-width along the n_b coordinate is controlled by the *transverse* filter, $w_t(n', \sigma')$, and the on-axis intensity profile is adjusted using the *longitudinal* window $w_l(\sigma')$. The design of the two functions is accomplished, via an iterative procedure, detailed in the full paper.

4 Example

In this example, we choose to synthesize a CB that follows a right-handed helical beam-axis with beam-width profile

$$W_b = 20\lambda \left(1 + 0.2sin(2\pi \frac{\sigma - \sigma_{\min}}{\sigma_{\max} - \sigma_{\min}})\right) \quad (6)$$

and on-axis intensity profile $I_b(\sigma) = 1$. The helical trajectory is described by

$$\mathbf{r}_b(\sigma) = [R(\cos\sigma - 1), R\sin\sigma, P\sigma],\ 0.5\pi \leq \sigma \leq 3\pi, \quad (7)$$

where R denotes the helix radius and the parameter P sets the pitch to be $2\pi P$. By setting $R = P = 20\lambda$ and following the procedure in section 3, we numerically calculate the phase aperture function $S(x', y')$ and the amplitude aperture function $A(x', y')$. Using this aperture design, we evaluate

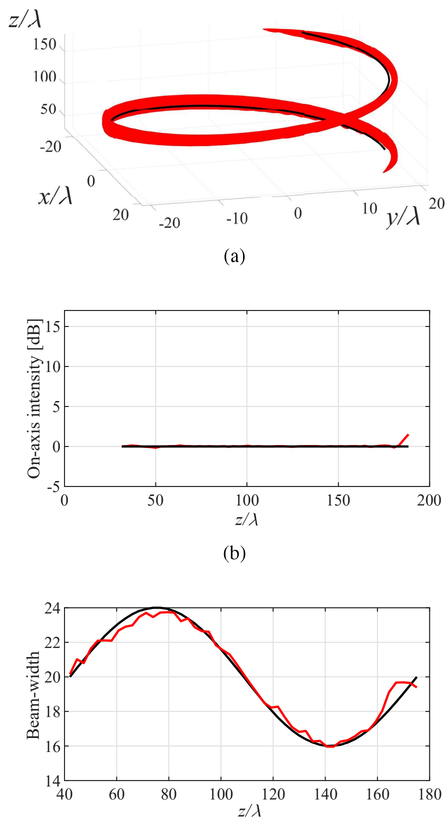

Figure 3. Control of the on-axis and off-axis intensity. (a) Iso-level surfaces of the -3dB of the CB maximum intensity in the $z > 0$ half-space (the desired trajectory is plotted in black line). (b) On-axis intensity profile of the CB (the desired profile in black line and the measured one in red). (c) Beam-width profile of the CB (the desired one in black and the measured one in red).

the intensity and plot in figure 3 the resulting iso-surfaces of the -3dB of the peak intensity 3(a), the on-axis intensity profile 3(b), and the beam-width in the $\hat{\mathbf{n}}_b$ direction 3(c). Clearly, the resulting intensity profile and beam width (red lines) follow the desired features $I(\sigma)$ and $W_b(\sigma)$ (black lines).

5 Conclusions and Future Research

The design of optimal aperture distributions that can produce arbitrary CBs involves various challenges. This paper addresses that of selecting the initial guess to facilitate convergence of aperture optimization schemes. This was achieved by constructing aperture distributions that correspond to CBs with desired trajectories, using a ray-based back-propagation technique. Basic control of the beam-width and the on-axis intensity profiles was achieved by employing an iterative correction scheme. Following this stage is the implementation of a suitable optimization technique that is required to address more complex design features.

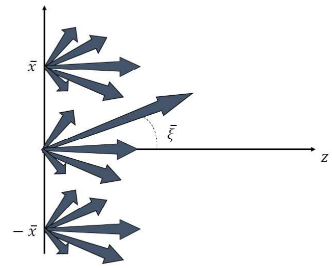

Figure 4. Gaussian beams decomposition of aperture fields. The field is described by the superposition of shifted and tilted Gaussian beam propagators that are emanating from a discrete spatial-directional lattice over the aperture.

Note that the optimization will not be performed directly on vectors comprising samples of the aperture field, as that will result in a large dimensionality variable-space and excessive computational costs. Instead, we plan to take advantage of the ray-field nature of the desired beam patterns, in order to construct the radiating field via a sparse basis of Gaussian beams, emanating from points in the aperture in different directions (Fig.4).

Finally, this work can be extended to other applications that involve field pattern manipulation, such as antenna array or near-field design. Another research avenue is on the extension for in-homogeneous media, which is of relevance to localized inverse scattering, geophysical applications, nondestructive evaluation methods, and beyond.

6 Acknowledgments

This research was supported by the ISRAEL SCIENCE FOUNDATION (grant No. 531/19).

References

[1] J. Baumgartl, M. Mazilu, and K. Dholakia, “Optically mediated particle clearing using airy wavepackets,” *Nat. Photonics*, vol. 2, pp. 675-678, Sept. 2008.

[2] S. Jia, J. C. Vaughan, and X. Zhuang, “Isotropic 3d super-resolution imaging with a self-bending point spread function,” *Nat. Photonics*, vol. 8, pp. 302-306, Mar. 2014.

[3] D. Kuang, Y. Cao, T. Lépine, and W. Mi, “Curved surface plasmon polariton excitation with shaped beam by fifth-power phase mask,” *IEEE Photonics J.*, vol. 7, no. 6, pp. 1-5, Dec. 2015.

[4] T. Vettenburg, H. I. C. Dalgarno, J. Nylk, C. Coll-Lladó, D. E. K. Ferrier, T. Cizmar, F.J. Gunn-Moore, and K. Dholakia, “Light-sheet microscopy using an

Airy beam," *Nat. Methods.*, vol. 11, pp. 541-544, Apr. 2014.

[5] M. Zhang, Z. Ren, and P. Yu, "Improve depth of field of optical tomography using finite energy Airy beam," *Opt. Lett.*, vol. 44, no. 12, pp. 3158-3161, June 2019.

[6] P. Polynkin, M. Kolesik, J. V. Moloney, G. A. Siviloglou, and D. N. Christodoulides, "Curved plasma channel generation using ultraintense Airy beams," *Science*, vol. 324, no. 5924, pp. 229-232, Apr. 2009.

[7] G. A. Siviloglou, J. Broky, A. Dogariu, and D. N. Christodoulides, "Observation of accelerating Airy beams," *Phys. Rev. Lett.*, vol. 99, no. 21, p. 213901, Nov. 2007.

[8] Y. Kaganovsky, and E. Heyman, "Wave analysis of Airy beams," *Opt. Express*, vol. 18, no. 1, pp. 8440-8452, Apr. 2010.

[9] T. Melamed, and A. Shlivinski, "Practical algorithm for custom-made caustic beams," *Opt. Lett.*, vol. 42, no. 13, pp. 2499-2502, June 2017.

[10] M. Born, and F. Wolf, *Principles of Optics*, Pergamon Press, New York, 1964.